Int. J. Electrochem. Sci., 14 **(2019)** 2732 – 2742, doi: 10.20964/2019.03.39

International Journal of
ELECTROCHEMICAL
SCIENCE
www.electrochemsci.org

Direct Electrochemistry and Electrocatalysis of Myoglobin with Copper Benzenetricarboxylate Metal-Organic Frameworks@ Nitrogen-Doped Graphene Composite Modified Electrode

Guiling Luo[1], *Ying Deng*[1], *Hui Xie*[1], *Juan Liu*[2], *Si Mi*[1], *Binghang Li*[1], *Guangjiu Li*[2], *Wei Sun*[1,*]

[1] Key Laboratory of Functional Materials and Photoelectrochemistry of Haikou, Key Laboratory of Laser Technology and Optoelectronic Functional Materials of Hainan Province, College of Chemistry and Chemical Engineering, Hainan Normal University, Haikou 571158, P R China
[2] Key Laboratory of Optic-electric Sensing and Analytical Chemistry for Life Science of Ministry of Education, College of Chemistry and Molecular Engineering, Qingdao University of Science and Technology, Qingdao 266042, P R China
[*]E-mail: sunwei@hainnu.edu.cn

Received: 19 November 2018 / *Accepted:* 11 January 2019 / *Published:* 7 February 2019

A novel nanohybrid material based on copper benzenetricarboxylate metal-organic framework (Cu-BTC) and nitrogen-doped graphene (NG) was used to immobilize myoglobin (Mb) with its biosensing ability checked. The surface images of the modifiers on the electrode were characterized by SEM. Spectroscopic results demonstrated that Mb kept its native structure in the composite film. Direct electrochemistry of Mb on Cu-BTC@NG modified electrode was checked by cyclic voltammetry with a pair of well-defined redox peaks observed. The peak-to-peak separation of 0.082 V and the formal peak potential of -0.187 V were calculated, corresponding to the realization of direct electrode transfer of Mb. Electrochemical investigations of Mb modified electrode were studied in detail. The modified electrode showed good sensitivity and wide linear range to the analysis of trichloroacetic acid and sodium nitrite. All the results demonstrated that is hybrid matrix exhibited a fast electron transfer pathway for the electron transfer of Mb.

Keywords: Copper benzenetricarboxylate metal-organic framework; nitrogen-doped graphene; myoglobin; direct electrochemistry

1. INTRODUCTION

Myoglobin (Mb) belong to small size heme protein that existed in muscle cells, which consists of a protoheme and one peptide chain with the functions of oxygen carrier and pro-oxidant in complex redox process in blood. Because of commercial availability and well-known structure with heme

center, direct electrochemistry of Mb is investigated to study electron transfer process of living systems [1,2]. However, electron transfer of redox enzymes is usually slow and the enzymes are irreversibly denatured on the conventional working electrode, which can be due to the three-dimensional macrostructures that hindering the reaction with electrode, or the adsorption and passivation on the electrode interface [3]. To realize direct electrochemical process and retain the electrocatalysis, various methods have been reported to enhance the electron transfer rate with different kinds of modifiers including nanomaterials, biomolecules and so on [4,5].

Metal-organic frameworks (MOFs) exhibit characteristic nanoporous lattice that compose of metal-containing nodes (metal ions/clusters) with organic linkers. Therefore various structural and chemical diversities have been devised [6]. MOFs have exhibited the advantages including structural tailor ability, high micro-pore volume, controlled porosity, big pore size, high crystallinity and high metal content with potentially valuable active sites [7,8]. Therefore MOFs have been applied in various fields including gas storage, gas absorption, energy conversion, catalysis, chemical sensor, biomedicine, imaging and detoxification [9,10]. Copper benzenetricarboxylate (Cu-BTC) MOFs are face-centered-cubic crystals, which are consisted of interconnected three-dimensional structure with big square-shaped pores. It has been reported that Cu-BTC has good thermal stability with the ability to chemical functionalization [11]. Li et al. achieved an electrochemical sensor base on copper-based MOFs and graphene (GR) composites for bisphenol A detection [12]. Dong et al. fabricated 2,4-dichlorophenol sensor with Cu-BTC, which showed the linear range from 0.04 to 1.0 μmol/L [13]. Saraf et al. constructed a Cu-MOF/reduced graphene oxide hybrid for supercapacitors and electrochemical nitrite sensor [14]. To our knowledge, the utilization of Cu-BTC based composite for redox protein electrochemistry has not been reported.

As two-dimensional nanosheet, GR draws much attention due to its fantastic and unique physicochemical properties [15]. A great deal of interests for biosensor applications have been used with GR and its various derivatives [16]. Doping is an easy way to modulate the properties of GR, and doped GR can reform its electron spin density, atomic charge density and increases surface active sites [17]. Nitrogen doped GR (NG) has the ability such as long-term durability and anti-poisoning as metal-free catalyst [18]. Wang et al. synthesized three dimensional NG for high-performance supercapacitor electrodes [19]. Sun utilized NG for the protein electrochemistry [20] and lead ion detection [21].

In this paper, Mb was fixed on a Cu-BTC@NG modified electrode with direct electron transfer of Mb investigated. Because of good film-forming ability and biocompatibility Nafion was employed to fix Mb/Cu-BTC@NG on the electrode. The constructed biosensor was applied to detect trichloroacetic acid (TCA) and nitrite (NO_2^-), which showed fast electron transfer and prominent catalytic ability. In conclusion, a new way for the preparation of electrochemical sensor was proposed with the construction procedure of Nafion/Mb/Cu-BTC@NG/CILE depicted in scheme 1.

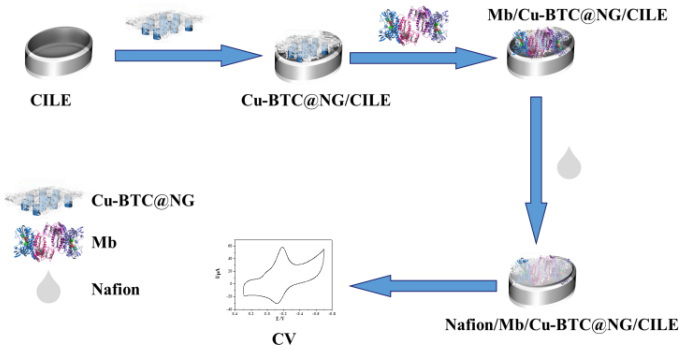

Scheme 1. Construction process of Nafion/Mb/Cu-BTC@NG/CILE.

2. EXPERIMENTAL

2.1 Apparatus and chemical

A computer-controlled electrochemical workstation (CHI 604E, Shanghai Chenhua Co., China) was used for cyclic voltammetry (CV) and electrochemical impedance spectroscopy (EIS) with three-electrode electrochemical system. Nafion/Mb/Cu-BTC@NG/CILE was acted as working electrode, saturated Ag/AgCl electrode as reference and Pt wire as the counter electrode. Ultraviolet-visible (UV-Vis) absorption spectrum was on TU-1901 spectrometer (Beijing Purkinje General Instrument, China). Fourier transform infrared (FT-IR) spectra were recorded on a Nicolet 6700 FT-IR spectrophotometer (Thermo Fisher Scientific Inc., USA). Scanning electron microscope (SEM) was performed on JSM-7100F scanning electron microscopy (Japan Electron Ltd. Co., Japan).

Equine skeletal muscle myoglobin (Mb, No. M-0630, Sigma-Aldrich, USA), Nafion polymer dispersions (wt% 5.0 ethanol solution, Beijing Honghaitian Tech. Co., China), 1-hexylpyridinium hexafluorophosphate ($HPPF_6$, Lanzhou Yulu Fine Chemicals, Co., China), Cu-BTC and NG (Nanjing XFNANO Materials Tech. Co., China), TCA (Tianjin Kemiou Chem., Co., China) and $NaNO_2$ (Shanghai Chem. Plant, China) were used directly. 0.1 mol/L phosphate buffer solution (PBS) were acted as supporting electrolyte. All chemicals were of analytical grade with solutions made up with twice-distilled water.

2.2 Fabrication of the Nafion/Mb/Cu-BTC@NG/CILE

CILE was home-made based on reference with $HPPF_6$ as the binder [22]. 1.0 mg Cu-BTC and 1.0 mg NG were dispersed into 1.0 mL water with 15 min ultrasonication to get a Cu-BTC@NG suspension. CILE was modified by a drop of 6.0 μL 1.0 mg/mL Cu-BTC@NG solution. A pipette tip was fitted on electrode to ensure water evaporated slowly in air to get uniform film on the electrode. 8.0 μL (15.0 mg/mL) Mb solutions was coated onto Cu-BTC@NG/CILE and dry in air. Lastly, 6.0 μL (0.5%) Nafion solution was casted on electrode to get the modified electrode (Nafion/Mb/Cu-BTC@NG/CILE).

3. RESULTS AND DISCUSSION

3.1 Spectroscopic results

The Soret absorption bands give data on conformational change of heme proteins region [23]. Fig. 1A showed the spectra of Mb in solution (curve a) and mixture of Mb with Cu-BTC@NG in solution (curve b), which exhibited the same Soret band at 408.5 nm, and that demonstrated the maintenance of Mb native structure within Cu-BTC@NG nanocomposite.

FT-IR spectroscopy was performed to prove the conformational integrity of heme proteins. The characteristic amide I (1700-1600 cm^{-1}, resulted from C=O stretching vibration of peptide linkages in the backbone of the protein) and amide II (1620-1500 cm^{-1}, a combination of N-H bending and C-N stretching vibrations) bands of proteins can provide the detailed data on the secondary structure of polypeptide chain. As shown in Fig. 1B, the amide I and II of Mb appeared at 1649 and 1529 cm^{-1} (curve a). The mixture of Cu-BTC@NG and Mb had wavenumbers at 1648 and 1529 cm^{-1} (curve b). The similar spectroscopic peaks proved that Mb still kept its native states after immobilized with Cu-BTC@NG.

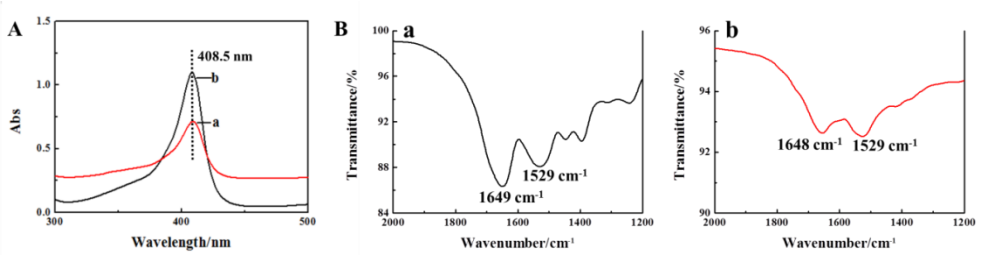

Figure 1. (A) UV-Vis absorption spectra of Mb (curve a) and Mb/Cu-BTC@NG mixture (curve b) with water; (B) FT-IR spectra of Mb (curve a) and Mb/Cu-BTC@NG (curve b).

3.2 SEM results

Fig. 2A displayed the SEM micrograph of Cu-BTC, which showed as irregularly cubic nanoparticles and appeared to certain agglomerate with rough surface. SEM image of NG nanosheets was consisted of the corrugated and scrolled sheets that resembled to typical crumpled silk veil waves (Fig. 2B). Fig. 2C and Fig. 2D exhibited the SEM images of Cu-BTC@NG nanocomposite, in which NG were mixed with densely packed and irregularly shaped Cu-BTC to form a composite.

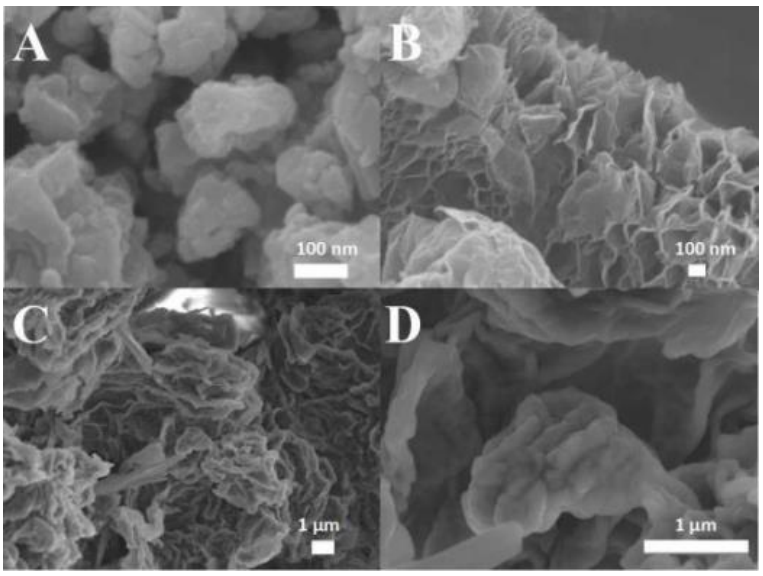

Figure 2. SEM images of Cu-BTC (A), NG (B), Cu-BTC@NG composite (C and D) at different magnifications.

3.3 Direct electrochemistry of Mb

Fig. 3A and B gave the typical CV of different modified electrodes. No voltammetric peak were found at Nafion/CILE (curve a) and Nafion/NG/CILE (curve c) in the potential window. The reduction peaks at -0.102 V of Nafion/Cu-BTC/CILE (curve b) and Nafion/Cu-BTC@NG/Nafion (curve d) were due to the presence of Cu-BTC. On Fig. 3B obvious redox peaks appeared at Nafion/Mb/CILE (curve e) and Nafion/Mb/Cu-BTC@NG/CILE (curve f), which illustrated that these peaks were attributed to the presence of Mb. Mb is a redox protein that can realized direct electron transfer at suitable conditions. Also the responses of curve f were bigger than that of curve e, showing the positive effects of Cu-BTC@NG to electron transfer.

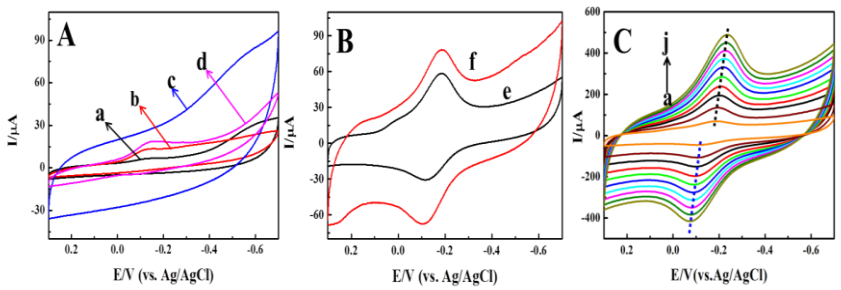

Figure 3. (A) CVs of (a) Nafion/CILE, (b) Nafion/Cu-BTC/CILE, (c)Nafion/NG/CILE, (d)Nafion/Cu-BTC@NG/CILE; (B) CVs of (e) Nafion/Mb/CILE and (f) Nafion/Mb/Cu-BTC@NG/CILE in PBS (pH 2.0) at scan rate of 100 mV/s. (C) CVs of Nafion/Mb/Cu-BTC@NG/CILE in a pH 2.0 PBS at different scan rate (from a to j: 100, 200, 300, 400, 500, 600, 700, 800, 900, 1000 mV/s).

The high microspores volume and excellent conductive of Cu-BTC@NG provided a suitable microenvironment for redox protein Mb to keep biological activity, facilitated the electron transfer between Mb and the electrode. As listed in table 1, electrochemical parameters of these Mb based electrodes were compared.

Table 1. Comparison of electrochemical parameters of different Mb modified electrodes.

Electrode	I*pc*/μA	I*pa*/μA	E*pc*/V	E*pa*/V	I*pc*/I*pa*	ΔE/V	$E^{0'}$
Nafion/Mb/CILE	18.97	21.91	-0.198	-0.114	0.866	0.085	-0.150
Nafion/Mb/Cu-BTC@NG/CILE	30.86	33.38	-0.187	-0.105	0.925	0.082	-0.146

Fig. 3C showed CV of Nafion/Mb/Cu-BTC@NG/CILE at different scan rate. In the scan rate of 100~1000 mV/s, the cathodic peak currents (I*pc*) and anodic peak currents (I*pa*) were linear to scan rate with regression equations of I*pc*(μA)=162.4υ(V/s)+18.09 (n=18, γ=0.990) and I*pa*(μA)=-143.5υ (V/s) -21.01 (n=18, γ=0.991). This result clarified that the electrochemical behavior of Nafion/Mb/Cu-BTC@NG/CILE belonged to a thin layer electrochemical behavior, as expect for electrode reaction adsorption control process [24]. The anodic peak potentials (E*pa*) moved to the positive direction with the cathodic peak potentials (E*pc*) to the negative direction at higher scan rate, which resulted in the increase of the peak-to-peak separation (ΔEp). When ΔEp>200 mV, a graph of E*pa* and E*pc* versus the logarithm of scan rate yielded two straight lines with the slopes of 2.3RT/(1−α)nF and -2.3RT/αnF [25]. The linear regression equations were E*pa*(V)=0.0578lnυ(V/s)-0.0695 (n=7, γ=0.996) and E*pc*(V) = -0.0434lnυ(V/s) -0.238 (n=7, γ=0.992), respectively. According to Laviron's theory and the calculation formula of quasi-reversible thin-layer electrochemical process [26, 27], electron transfer coefficient (α) and transferred electron (n) were obtained to be 0.56 and 1.04 from the slopes. According to the formula for reaction rate constant (*ks*), $\log k_S = \alpha \log(1-\alpha) + (1-\alpha)\log\alpha - \log\frac{RT}{nF\upsilon} - (1-\alpha)\alpha\frac{nF\Delta Ep}{2.3RT}$, k_s value was calculated to be 0.817 s^{-1}.

3.4 Effect of buffer pH

In general the electrochemical behavior of redox proteins is often influenced by the buffer pH. Fig. 4 showed the CVs of Nafion/Mb/Cu-BTC@NG/CILE in PBS at different pH values. As can be seen, nearly reversible redox peaks were obtained in the pH range of 2.0~8.0 and peak potentials shifted negatively with the increase of pH. Plot of the formal potential versus pH gave the equation as $E^{0'}$(V)=-0.0474 pH-0.0074 (n=4, γ=0.996). The slope value (47.4 mV/pH) was small than the theoretical value (59 mV/pH) of the reversible proton-coupled single electron transfer at 298 K. The results showed that Mb occurred one electron and one proton transfer process as Mb Fe (III)+H^++e^- →Mb Fe (II) [24]. The maximum peak current was achieved in pH 2.0 PBS, which was used for the following investigation.

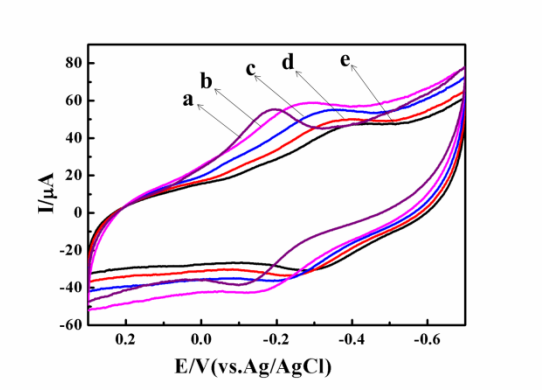

Figure 4. CVs of Nafion/Mb/Cu-BTC@NG/CILE in different pH PBS (from a to g: 2.0, 4.0, 6.0, 7.0, 8.0) at 100 mV/s.

3.5 Electrocatalysis to TCA reduction

Electrocatalytic behavior of this Mb modified electrode to TCA reduction was investigated. Fig. 5 was CVs of Nafion/Mb/Cu-BTC@NG/CILE in PBS (pH 2.0) with different amounts of TCA. The increases of TCA concentration resulted in the increase of the reduction current with a new reduction peak appeared at -0.256 V, while the oxidation peak decreased slowly or even disappeared. The inset of Fig. 5 showed the linear relationship of the electrocatalytic reduction current and the TCA concentration from 1.0 to 460.0 mmol/L. The linear equation was I*pc*(μA)=2.621±0.137C (mmol/L)+38.63±0.28 (n=16, γ=0.999) with the detection limit as 0.333 mmol/L (3σ). The apparent Michaelis-Menten constant (K_M^{app}) can be obtained with the following Lineaweaver-Burk form of the Michaelis-Menten equation and the result was 13.88 mmol/L.

$$\frac{1}{I_{ss}} = \frac{1}{I_{\max}} + \frac{K_M^{app}}{I_{\max} C}$$

Here I_{ss} is the steady-state current after the addition of TCA; I_{max} is the maximum current under saturated TCA solution; C is the bulk concentration of TCA. This result demonstrated that the large specific area and good conductivity of Cu-BTC@NG increased the amount of Mb on the electrode surface, accelerated the electron transfer rate between Mb and the electrode, and improved the electrocatalytic performance of the electrode. A comparison of the electrochemical and analytical parameters of this biosensor with other Mb modified electrodes was summarized in table 2.

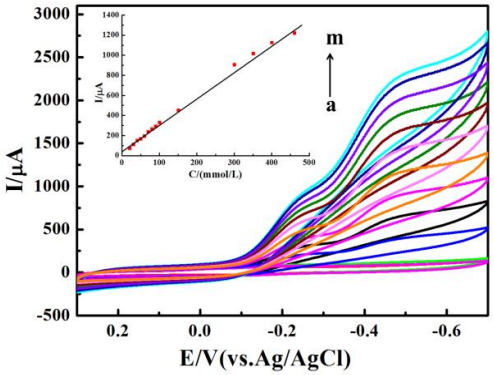

Figure 5. CVs of Nafion/Mb/Cu-BTC@NG/CILE with 0, 1, 5, 50, 100, 150, 200, 250, 300, 350, 400, 450, 460 mmol/L TCA (a to m) in pH 2.0 PBS at the scan rate of 100 mV/s. Inset was linear relationship of catalytic reduction currents and the TCA concentration.

Table 2. Comparison of electrochemical parameters of different Mb modified electrodes to TCA detection.(*n*=3)

Modified electrodes	Linear range (mmol/L)	Detection limit (mmol/L)	K_M^{app} (mmol/L)	Refs.
Nafion/Mb-SA-TiO_2/CILE	5.3-114.2	0.152	32.3	[28]
Nafion/Mb/Co/CILE	0.4-12.0	0.2	4.11	[29]
Mb/ZrPNS/GCE	0.1–2.2	0.025	5.6	[30]
CTS-Mb-GR-IL/CILE	2.0-16.0	0.583	8.99	[31]
Mb-agarose/GCE	No given	No given	177.0	[32]
Nafion/Mb/NiO/GR/CILE	0.69-30.0	0.23	10.67	[33]
Mb-HSG-SN-CNTs/GCE	0.002-1.2	0.0036	1.62	[34]
Nafion/Mb/Cu-BTC@NG/CILE	1.0-460	0.333	13.88	This Work

3.6 Electrocatalysis to nitrite reduction

Fig. 6 showed the CVs of Nafion/Mb/Cu-BTC@NG/CILE towards the reduction of NO_2^- at 0.1 mol/L pH 2.0 PBS. A new reduction peak appeared at -0.554 V with the peak currents increased gradually. Inset of Fig. 6 gave the linear relationship of the reduction current and the NO_2^- concentration in the range from 0.01 mmol/L to 2.6 mmol/L with a linear equation of I*pc*(μA)=90.22± 0.23C (mmol/L) +61.12±0.35 (n=11, γ=0.997). The detection limit was 3.3 μmol/L (3σ). Furthermore, when the concentration of NO_2^- was higher than 2.6 mmol/L, a response plateau was reached. The K_M^{app} value was calculated according to the Lineaweaver-Burk equation with the result as 2.0 mmol/L. Also a comparison of the electrochemical parameters for the detection of $NaNO_2$ with different Mb modified electrodes was summarized in table 3.

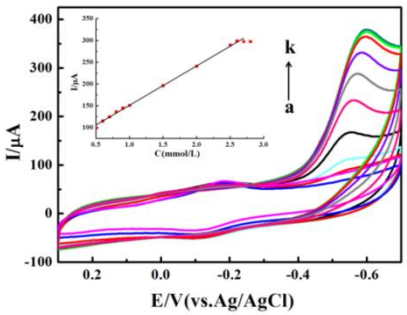

Figure 6. CVs of Nafion/Mb/Cu-BTC@NG/CILE with 0, 0.01, 0.1, 0.2, 0.5, 1.0, 1.5, 2.0, 2.5, 2.6, 2.8 mmol/L NO_2^- (a to k) in pH 2.0 PBS at the scan rate of 100 mV/s. Inset was linear relationship of catalytic reduction currents and the NO_2^- concentration.

Table 3. Comparison of electrochemical parameters of different Mb modified electrodes to $NaNO_2$ detection (*n*=3).

Modified electrodes	Linear range (mmol/L)	Detection limit (mmol/L)	K_M^{app} (mmol/L)	Refs.
Mb/ZrPNS/GCE	3.0–800.0	0.66	No given	[30]
CTS/SWCNHs/CILE	0.04-0.74	0.13	8.99	[35]
CTS/TiO_2-Hb/CILE	0.8-20.0	0.26	3.66	[36]

SA-Mb-IL-Fe_2O_3/CILE	4.0-140	1.30	27.60	[37]
SG-Ag_{nps}/GCE	0.004-0.048	0.0040	No given	[38]
Nafion/Mb/Cu-BTC@NG/CILE	0.01-2.6	0.0033	2.00	This Work

3.7 Stability

The stability of Nafion/Mb/Cu-BTC@NG/CILE was investigated by continuous cyclic voltammetric scanning. After scanned for 250 cycles at 100 mV/s, no obvious changes appeared. Six electrodes were fabricated independently, which gave an acceptable RSD of 0.97±0.04% for the analysis of 20.00 mmol/L TCA.

3.8 Applications in sample analysis

Various samples were detected by the proposed methods. The TCA content in the medical skin lotion (35% TCA, Shanghai EKEAR Bio. Tech. Co., China) was tested. Pickled vegetables were brought from farm product market and the soak water was got by filtering dreg out of the mixture before usage for the determination of $NaNO_2$. The concentration of the analyte in the sample solution was calculated by the calibration curve. As shown in table 4, the recovery was determined by adding the standard TCA or $NaNO_2$ solution to the samples, which gave the values between 98.55% and 99.69% for TCA and 104.3% for $NaNO_2$. It was proved that this Mb modified electrode had good catalytic effect to TCA or $NaNO_2$ and could be used to the real samples detection.

Table 4. Analytical data of TCA and $NaNO_2$ concentration in real samples by the proposed method. (n=3)

Sample	Detected (mmol/L)	Added (mmol/L)	Total (mmol/L)	Recovery (%)
Medical facial peel solution for TCA	20.95	10.00	30.85	99.69
		20.00	40.35	98.55
		30.00	50.35	98.82
Soak water from pickled vegetables for $NaNO_2$	ND	0.46	0.48	104.3

4. CONCLUSION

In this experiment Cu-BTC@NG was used as new modifier for the construction of Mb based electrochemical sensor, which was successfully applied in sensing of TCA and NO_2^-. Cu-BTC@NG composite exhibited a porous structure, which facilitated the electron transfer between Mb and the substrate CILE. Nafion/Mb/Cu-BTC@NG/CILE showed excellent electrocatalytic detection of NO_2^- and TCA with satisfactory results. Various samples were analyzed, which proved the potential applications of Cu-BTC@NG composite.

ACKNOWLEDGEMENT
This project was financially supported by the Hainan Province National Natural Science Foundation of China (2017CXTD007), the Key Science and Technology Program of Haikou City (2017042), Graduate Student Innovation Research Project of Hainan Province (Hys2018-212) and Research Fund from Beijing Innovation Center for Future Chips (KYJJ2018006).

References

1. S. I. Rao, A. Wilks, M. Hamberg and P. R. Ortiz de Montellano, *J. Biol. Chem.*, 269(1994)7210
2. I. Hamachi, S. Noda and T. Kunitake, *J. Am. Chem. Soc.*, 113(1991)9625
3. G. C. Zhao, L. Zhang, X. W. Wei and Z. S. Yang, *Electrochem. Commun.*, 5(2003)825
4. G. Zhao, J. J. Xu and H. Y. Chen, *Electrochem. Commun.*, 8(2006)148
5. M. Hasanzadeh, N. Shadjou and M. D. L. Guardia, *TrAC, Trends Anal. Chem.*, 89(2017)119.
6. A. K. Cheetham, C. N. R. Rao and R. K. Feller, *Chem. Commun.*, 46(2006)4780
7. G. Maurin, C. Serre, A. Cooper and G. Féreyd, *Chem. Soc. Rev.*, 46(2017)3104
8. D. J. Tranchemontagne, J. L. Mendoza-Cortés, M. O'Keeffe and O. M. Yaghi, *Chem. Soc. Rev.*, 38(2009)1257
9. S. Kempahanumakkagari, K. Vellingiri, A. Deep, E. E. Kwon, N. Bolan, and K. H. Kim, *Coord. Chem. Rev.*, 357(2018)105
10. J. W. Zhou and B. Wang, *Chem. Soc. Rev.*, 46(2017)6927
11. S. M. F. Lo and S. S. Y. Chui, *Science*, 283(1999)1148
12. C. M. Li, Y. L. Zhou, X. Zhu, B. X. Ye and M. T. Xu, *Int. J. Electrochem. Sci.*, 13(2018)4855
13. S. Y. Dong, G. C. Suo, N. Li, Z. Chen, L. Peng, Y. L. Fu, Q. Yang and T. L. Huang, *Sens. Actuators, B*, 222(2016)972
14. M. Saraf, R. Rajak and S. M. Mobin, *J. Mater. Chem. A.*, 4(2016)16432
15. K. S. Novoselov, S. V. Morozov, T. M. G. Mohinddin, L. A. Ponomarenko, D. C. Elias, R. Yang, I. I. Barbolina, P. Blake, T. J. Booth, D. Jiang, J. Giesbers, E. W. Hill and A. K. Geim, *Phys. Status. Solidi.*, 244(2010)4106
16. Y. Y. Shao, J. Wang, H. Wu, J. Liu, A. I. Aksay and Y. H. Lin, *Electroanalysis*, 22(2010)1027
17. Y. W. Zhang, J. Ge, L. Wang, D. H. Wang, F. Ding, X. M. Tao and W. Chen, *Sci. Rep.*, 3(2013): 2771
18. L. T. Qu, Y. Liu, J. B. Baek and L. M. Dai, *ACS nano*, 4(2010)1321
19. B. H. Wang, Y. Qin, W. S. Tan, Y. X. Tao and Y. Kong, *Electrochim. Acta*, 241(2017)1
20. W. Sun, L. F. Dong, Y. Deng, W. C. Wang and Q. Q. Zhu, *Mater. Sci. Eng., C*, 39(2014)86
21. Z. R. Wen, X. L. Niu, L. J. Yan, Y. Y. Niu, D. Wang, Z. F. Shi and L. F. Dong, *Int. J. Electrochem. Sci.*, 11(2016)6648
22. W. C. Wang, X. Q. Li, X. H. Yu, L. J. Yan, Z. F. Shi, X. Y. Wen and W. Sun, *J. Chin. Chem. Soc.*, 63(2016)298
23. P. George and G. Hanania, *Biochem. J.*, 55(1953)236
24. R. W. Murray and A. J. Bard, *J. Electroanal. Chem.*, 13(1984)191
25. X. J. Zhao, Z. B. Mai, X. H. Kang, Z. Dai and X. Y. Zou, *Electrochim. Acta*, 53(2008)4732
26. E. Laviron. *J. Electroanal. Chem.*, 52(1974)355
27. E. Laviron. *J. Electroanal. Chem.*, 101(1979)19
28. H. Q. Yan, X. Q. Chen, Z. F. Shi, Y. H. Feng, J. C. Li, Q. Lin, X. H. Wang and W. Sun, *J. Solid State Electrochem.*, 20(2016)1783
29. W. Sun, X. Q. Li, P. Qin and K.Jiao, *J. Phys. Chem. C.*, 113(2009)11294
30. Y. H. Zhang, X. Chen and W. S. Yang, *Sens. Actuators, B.*, 130(2008)682
31. C.X. Ruan, T. T. Li, Q. J. Niu, M. Lu, J. Lou, W. M. Gao and W. Sun, *Electrochim. Acta*, 64(2012)183
32. S. F. Wang, T. Chen, Z. L. Zhang, X. C. Shen, Z. X. Lu, D. W. Pang and K. Y. Wong, *Langmuir*,

21(2005)9260
33. W. Sun, S. X. Gong, Y. Deng, T. T. Li, Y. Cheng, W. C. Wang and L. Wang, *Thin Solid Films*, 562(2014)653
34. C. Y. Liu and J. M. Hu, *Biosens. Bioelectron.*, 24(2009)2149
35. L.J.Yan, X. L Niu, Z. R Wen, X. Y. Li, X. B. Li and W. Sun, *Int. J. Electrochem. Sci.*, 11(2016)8972
36. F. Shi, W.C. Wang, S.X. Gong, B.X. Lei, G.J. Li, X.M. Lin, Z.F. Sun and W. Sun, *J. Chin. Chem. Soc.*, 62(2015)554
37. T. R. Zhan, M. Y. Xi, Y.Wang, W. Sun and W. G. Hou, *J. Colloid Interface Sci.*, 346(2010)188
38. G. Maduraiveeran, P. Manivasakan and R. Ramaraj, *Int. J. Nanotechnol.*, 8(2011)925